Radiology: Cardiothoracic Imaging

ORIGINAL RESEARCH

Prognostic Value of Myocardial Parametric Mapping in Patients with Acute Myocarditis: A Retrospective Study

Yining Wang, PhD[*1] • *Xuejing Duan, MD*[*2] • *Leyi Zhu, PhD*[1] • *Jing Xu, MD*[1] • *Di Zhou, MD*[1] • *Wenjing Yang, PhD*[1] • *Mengdi Jiang, PhD*[1] • *Huaying Zhang, PhD*[1] • *Arlene Sirajuddin, MD*[3] • *Andrew E. Arai, MD*[4,5] • *Shihua Zhao, MD, PhD*[1] • *Hongyue Wang, MD*[**2] • *Minjie Lu, MD, PhD*[**1,6]

* Y.W. and X.D. contributed equally to this work.

** H.W. and M.L. are co–senior authors.

Author affiliations, funding, and conflicts of interest are listed at the end of this article.

Radiology: Cardiothoracic Imaging 2025; 7(1):e240125 • https://doi.org/10.1148/ryct.240125 • Content codes: CA MR

Purpose: To investigate the prognostic value of T1 mapping, extracellular volume fraction (ECV), and T2 mapping in a large cohort of patients with acute myocarditis.

Materials and Methods: This retrospective study included patients with acute myocarditis who underwent cardiac MRI (3.0 T) between March 2016 and October 2022. Diagnosis was confirmed by diagnostic cardiac MRI criteria or endomyocardial biopsy. The primary end point was major adverse cardiovascular events (MACEs), defined as the composite of cardiac death, heart failure hospitalization, heart transplantation, sustained ventricular arrhythmia, and recurrent myocarditis. Univariable and multivariable Cox regression analyses were performed to assess the association of clinical and cardiac MRI variables with the primary end point. The prognostic value of each model was assessed using the Harrell C index.

Results: A total of 235 patients (mean age, 32 years ± 13 [SD]; 150 [63.8%] men) were included. During a mean follow-up of 1637 days (IQR: 1441–1833 days), MACEs occurred in 45 (19%) patients. Patients with MACEs had higher global native T1, ECV, and T2 values (1342 msec ± 64 vs 1263 msec ± 48; $P < .001$; 39.1% ± 8.7 vs 32.7% ± 5.7; $P < .001$; 61.1 msec ± 10.0 vs 55.3 msec ± 9.4; $P = .03$, respectively). In a series of multivariable Cox regression models, native T1 (per 10-msec increase: hazard ratio, 1.61; 95% CI: 1.31, 1.98; $P < .001$) and ECV (per 5% increase: hazard ratio, 1.70; 95% CI: 1.38, 2.08; $P < .001$) independently predicted MACE occurrence, and the addition of native T1 (Harrell C index = 0.76) or ECV (Harrell C index = 0.79) to the model including only clinical variables, left ventricular ejection fraction, and septal late gadolinium enhancement (Harrell C index = 0.72) improved discrimination for the primary end point.

Conclusion: Cardiac MRI–derived native T1 and ECV were independent predictors of MACEs in patients with acute myocarditis and provided incremental prognostic value when combined with conventional parameters.

Supplemental material is available for this article.

Myocarditis is a multifaceted, heterogeneous heart disease that has received widespread attention in recent years. Patients may be asymptomatic or present with chest pain, dyspnea, palpitations, and even severe heart failure and ventricular tachycardia (1). Long-term follow-up studies showed that acute myocarditis progresses to dilated cardiomyopathy in about one in five patients and results in death in 1%–7% of patients (1,2).

Development of the 2018 Lake Louise criteria has led to an increase in the number of identified myocarditis cases (3), and more research is needed to gain a deeper understanding of the disease to improve risk stratification and optimal management. The main prognostic factor currently recognized is late gadolinium enhancement (LGE) at cardiac MRI, with several large cohort studies demonstrating an association between the degree, distribution, and location of enhancement with clinical outcomes (4–6). However, two large meta-analyses (4,5) demonstrated substantial heterogeneity in the proportion of patients with myocarditis presenting with LGE, ranging from 28.3% to 100%. In addition, LGE, as a semiquantitative technique for myocardial injury or necrosis, cannot accurately detect myocardial edema and interstitial fibrosis caused by myocarditis, which are known to greatly contribute to patient outcomes (7). In contrast, myocardial parametric mapping, such as T1 mapping, extracellular volume fraction (ECV), and T2 mapping, has become an essential part of the Lake Louise criteria and has demonstrated excellent diagnostic performance (3,8). It provides a more sensitive and quantitative assessment of myocardial changes by depicting small histologic alterations in the myocardium compared with conventional methods such as LGE. Without the need for comparison with the healthy remote myocardium and invasive procedures, parametric mapping allows early detection of inflammation and edema, which is essential for early diagnosis and rapid intervention (7,9). This advance represents a critical shift in the management and understanding of myocarditis, highlighting the need for further research into these novel diagnostic tools.

Several studies evaluating the prognostic value of cardiac MRI parametric mapping in patients with myocarditis have been published, providing us with valuable insights (10–12). However, these studies are limited by small sample sizes and lack of robust analyses for risk assessment, such as Cox regression analyses. Therefore, this study aims to further explore the role of myocardial parametric mapping in predicting the prognosis of patients with myocarditis.

Abbreviations

ECV = extracellular volume fraction, HR = hazard ratio, LGE = late gadolinium enhancement, LV = left ventricle, LVEF = LV ejection fraction, MACE = major adverse cardiovascular events

Summary

In patients with acute myocarditis, cardiac MRI–derived native T1 and extracellular volume fraction provided incremental prognostic value for predicting occurrence of major adverse cardiovascular events when combined in a model with conventional clinical and imaging parameters.

Key Points

- In a retrospective study of 235 patients with acute myocarditis, cardiac MRI–derived global native T1, extracellular volume fraction (ECV), and T2 values were significantly higher in patients with versus patients without major adverse cardiovascular events (1342 msec ± 64 [SD] vs 1263 msec ± 48; $P < .001$; 39.1% ± 8.7 vs 32.7% ± 5.7; $P < .001$; 61.1 msec ± 10.0 vs 55.3 msec ± 9.4; $P = .03$, respectively).
- Native T1 (per 10-msec increase: hazard ratio, 1.61; 95% CI: 1.31, 1.98; $P < .001$) and ECV (per 5% increase: hazard ratio, 1.70; 95% CI: 1.38, 2.08; $P < .001$) were independent predictors of major adverse cardiovascular events at multivariable Cox regression analysis.
- The addition of native T1 (Harrell C index = 0.76) and ECV (Harrell C index = 0.79) to the multivariable model including only standard clinical and imaging variables (Harrell C index = 0.72) resulted in improved prognosis prediction.

Keywords

MRI, Cardiac, Heart, Inflammation

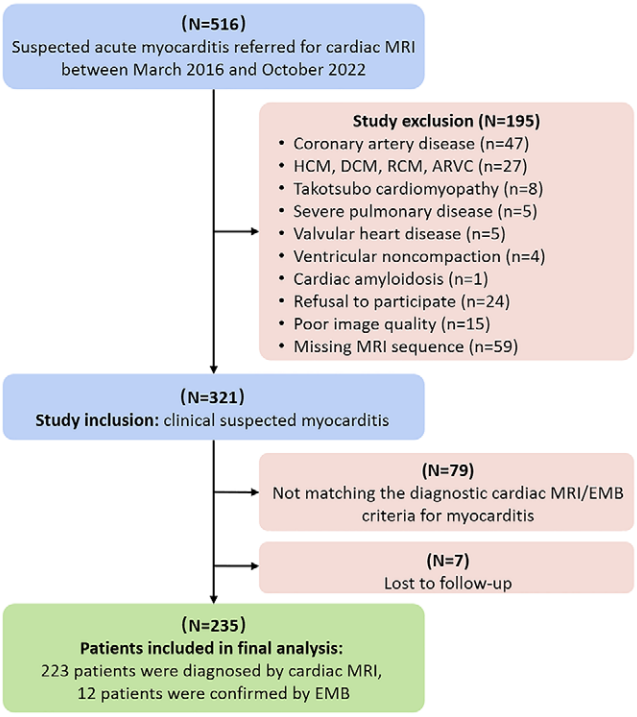

Figure 1: Flowchart of patient selection process based on inclusion and exclusion criteria. ARVC = arrhythmogenic right ventricular cardiomyopathy, DCM = dilated cardiomyopathy, EMB = endomyocardial biopsy, HCM = hypertrophic cardiomyopathy, RCM = restrictive cardiomyopathy.

Materials and Methods

Study Sample

This retrospective study included consecutive patients with acute myocarditis who underwent cardiac MRI between March 2016 and October 2022. The study was approved by the ethics committee of Fuwai Hospital (no. 2022–1770), and the requirement for informed consent was waived.

The inclusion criteria were based on the clinical and imaging diagnostic criteria given by the 2013 European Society of Cardiology position statement (13) and criteria used in previous publications (14,15): clinical presentations of myocarditis, including acute chest pain, chest tightness, new-onset or worsening dyspnea, unexplained arrhythmia symptoms, and/or syncope or unexplained cardiogenic shock; diagnostic factors, including abnormal 12-lead electrocardiogram, elevated high-sensitivity cardiac troponin I level, and functional and structural abnormalities at US imaging; and myocarditis ascertained through endomyocardial biopsy or diagnostic cardiac MRI criteria. Myocarditis was diagnosed by 2018 Lake Louise criteria when at least one T2-based criterion (increased myocardial T2 relaxation times or increased T2 signal intensity ratio) and at least one T1-based criterion (increased myocardial T1, ECV, or LGE) were present. Patients were excluded if they had any evidence of coronary artery disease (coronary stenosis > 50% proven by angiography) and/or other pre-existing cardiac disease or systemic disease with interpretable symptoms, including hypertrophic cardiomyopathy, cardiac amyloidosis, arrhythmogenic right ventricular cardiomyopathy, takotsubo cardiomyopathy, ventricular noncompaction, valve disease, and pulmonary embolism (Fig 1).

Cardiac MRI Protocol and Analysis

All patients underwent cardiac MRI with a 3.0-T scanner using a standardized, routine imaging protocol. Cardiac morphologic and functional parameters were assessed using electrocardiographically gated, breath-hold, cine steady-state free precession acquisitions in three long-axis planes and the short-axis plane. On the short-axis images, a complete series of sections containing the left ventricle (LV) were acquired from apex to base (section thickness: 8 mm; gap: 2 mm; repetition time: 2.9–3.4 msec; echo time: 1.5–1.7 msec; matrix size: 192 × 224–224 × 256; and field of view: 320–380 mm).

LGE images were obtained starting at 10–15 minutes after administration of a contrast agent (0.2 mmol/kg, gadopentetate dimeglumine, Magnevist, Bayer Healthcare) by using a gradient spoiled fast low-angle shot sequence with phase-sensitive inversion recovery technique. LGE was performed in four- and two-chamber view and a series of contiguous 6-mm LV short-axis sections that covered the entire LV. The inversion time was individually assessed per patient to null the myocardial signal. Edema-sensitive T2-weighted short tau inversion recovery sequences were performed on short-axis and four-chamber views (repetition time: two R-R intervals to ensure repetition time ≥ 1500 msec; echo time: 80 msec; field of view: 300–380 mm; matrix: 160 × 143; and voxel size: 2.0 × 2.0 × 8 mm).

T1 and T2 mapping were acquired in two long-axis (four- and two-chamber) views and three short-axis views of the LV (basal, midventricular, and apical). Native and postcontrast T1 quantification was performed with modified Look-Locker inversion recovery sequence during a breath hold, followed by the 5(3)3

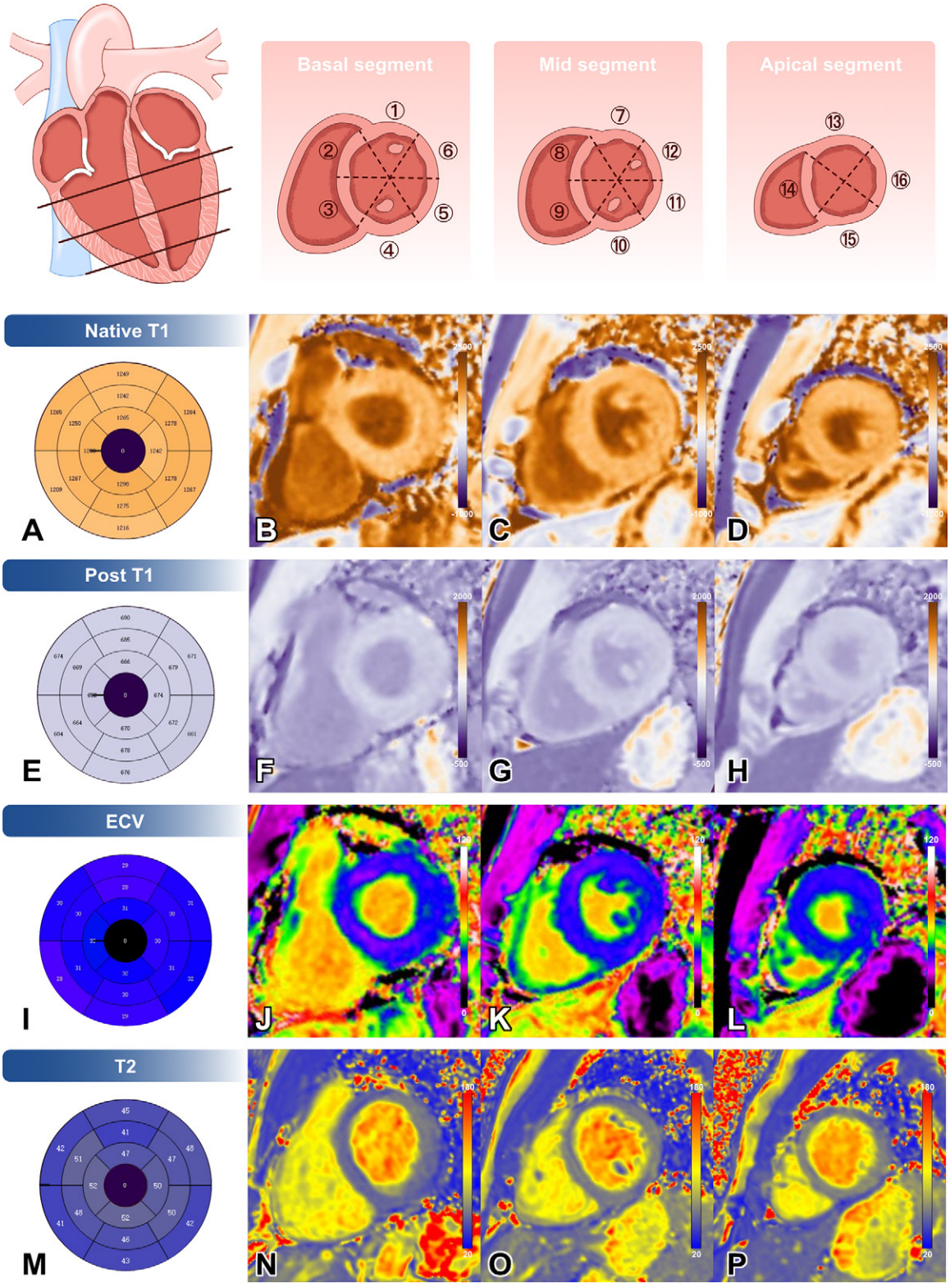

Figure 2: Measurement and bull's-eye diagram of native T1 **(A)**, postcontrast (post) T1 **(E)**, extracellular volume fraction (ECV) **(I)**, and T2 **(M)**. Representative left ventricular short-axis images of native T1 mapping **(B–D)**, postcontrast T1 mapping **(F–H)**, ECV **(J–L)**, and T2 mapping **(N–P)**.

and 4(1)3(1)2 protocols, respectively (16,17). The typical T1 mapping imaging parameters were as follows: matrix: 162 × 256; section thickness: 6 mm; and repetition time/echo time: 2.5/1.0 msec. T2 mapping was acquired in a six-echo gradient spin-echo sequence at the same short-axis positions corresponding to T1 mapping, which included basal, mid, and apical LV (11,18).

Cardiac MRI studies were analyzed independently by two observers (M.L., with 19 years of experience with cardiac MRI, and Y.W., with 3 years of experience with cardiac MRI) while blinded to the clinical information and prognosis of all patients. All postprocessing and image analysis was carried out using commercially available software (Medis, version 4.0; Medis Medical

Table 1: Patient Characteristics

Parameter	All Patients (*n* = 235)	Group with MACEs (*n* = 45)	Group without MACEs (*n* = 190)
Demographics			
Age (y)	32 ± 13	35 ± 14	31 ± 13
Sex			
Male	150 (63.8)	26 (58)	124 (65.3)
Female	85 (36.2)	19 (42)	66 (34.7)
Body mass index	23.7 ± 4.3	23.4 ± 4.1	23.8 ± 4.3
Heart rate (beats/min)	73 ± 15	76 ± 16	72 ± 14
Cardiovascular risk factors			
Hypertension	33 (14.0)	7 (16)	26 (13.7)
Diabetes mellitus	11 (4.7)	4 (9)	7 (3.7)
Smoking	65 (27.7)	9 (20)	56 (29.5)
NYHA functional class			
I–II	155 (66.0)	20 (44)	135 (71.1)
III–IV	80 (34.0)	25 (56)	55 (28.9)
Clinical presentation			
Infarctlike presentation	110 (46.8)	10 (22)	100 (52.6)
Heart failure presentation	87 (37.0)	27 (60)	60 (31.6)
Arrhythmia presentation	38 (16.2)	8 (18)	30 (15.8)
Laboratory tests			
hs-cTnI (ng/mL)	0.066 (0.017–0.404)	0.128 (0.043–0.778)	0.064 (0.014–0.317)
C-reactive protein (mg/L)	6.050 (2.360–13.700)	5.0 (2.3–10.1)	6.5 (2.5–15.6)
NT-proBNP (pg/mL)	363.5 (79.4–1316.0)	1300.5 (540.1–3312.3)	240.0 (72.3–844.3)
Log NT-proBNP	2.5 ± 0.8	3.0 ± 0.9	2.4 ± 0.8
MYO (ng/mL)	20.6 (12.2–38.8)	29.1 (11.5–56.4)	19.9 (12.1–35.8)
CK-MB (ng/mL)	1.6 (0.8–5.5)	2.4 (1.3–9.8)	1.5 (0.8–5.3)
NEUT (%)	65.9 ± 13.0	67.2 ± 13.7	65.6 ± 12.8
HCT (%)	41.6 ± 5.2	41.4 ± 5.5	41.6 ± 5.2
WBC (10^3/μL)	8.6 ± 3.4	9.9 ± 3.8	8.3 ± 3.3
Time interval between symptom onset and cardiac MRI (d)	13 (7–20)	14 (8–21)	13 (7–20)

Note.—Data are presented as means ± SDs, medians with IQRs in parentheses, or numbers of patients with percentages in parentheses. Body mass index is calculated as weight in kilograms divided by height in meters squared. CK-MB = creatine kinase MB isoenzyme, HCT = hematocrit, hs-cTnI = high-sensitivity cardiac troponin I, MACE = major adverse cardiovascular event, MYO = myoglobin, NEUT = neutrophil percentage, NT-proBNP = N-terminal pro–brain natriuretic peptide, NYHA = New York Heart Association, WBC = white blood cell.

Imaging). Linear dimensions of the cardiac chambers (left atrium dimension and LV end-diastolic diameter) and LV volumes (LV end-diastolic volume, LV end-systolic volume, stroke volume, cardiac output, LV mass, and left ventricular ejection fraction [LVEF]) were measured in the standard manner (19). LV end-diastolic volume, LV end-systolic volume, LV mass, and LV ejection fraction were then calculated, and volumes were adjusted for body surface area and expressed as indexes. Papillary muscles and trabeculae were included in the LV volumes and excluded from LV mass. Epicardial and endocardial contours of LV were manually traced on short-axis LGE images, and areas of signal intensity greater than 5 SDs from normal myocardium were defined as LGE (15). The LGE extent was expressed as the percentage of total LV myocardial mass. LV endocardial and epicardial borders on cine images were manually contoured to define the myocardium. Using the right ventricular insertion point as a reference, T1, ECV, and T2 maps were segmented according to the American Heart Association 16-segment model (apex excluded) (17). Native T1 and T2 value measurements in each of the 16 segments were automatically calculated with commercially available software, with global values provided as the average of all segments (Fig 2). ECV, a marker of interstitial contrast agent accumulation, was calculated using T1 measurements of myocardium and blood pool before and after contrast material administration and hematocrit value (20). The native T1, ECV, and T2 values were converted into dichotomous variables according to the cutoff values of 2 SDs above the mean of the reference range, and patients with 2*n* times SD of the normal range were classified as high risk for major adverse cardiovascular events (MACEs) (21,22).

Primary End Point

The identification of composite end point events was based on the electronic medical record system of Fuwai Hospital or telephone

Table 2: Cardiac MRI Characteristics

Parameter	All Patients (*n* = 235)	Group with MACEs (*n* = 45)	Group without MACEs (*n* = 190)	*P* Value
Cardiac MRI quantification of function and structure				
LAD (mm)	28.2 ± 7.9	34.5 ± 9.3	26.8 ± 6.8	<.001
LVEDD (mm)	51.7 ± 8.0	54.8 ± 8.8	50.9 ± 7.5	.002
LVEF (%)	50.9 ± 14.1	39.4 ± 16.5	53.6 ± 12.0	<.001
LVEDVi (mL/m^2)	87.1 ± 31.1	105.8 ± 42.0	82.6 ± 26.2	.001
LVESVi (mL/m^2)	45.5 ± 30.3	69.0 ± 41.4	39.9 ± 24.0	<.001
LVSV (mL)	74.3 ± 22.7	62.9 ± 20.2	77.0 ± 22.5	<.001
LVCI (L/min/m^2)	3.0 ± 0.8	2.7 ± 0.7	3.0 ± 0.8	.01
LVCO (L/min)	5.3 ± 1.7	4.6 ± 1.5	5.5 ± 1.7	.002
Left ventricle mass (g)	91.3 ± 30.0	86.6 ± 24.7	92.4 ± 31.1	.24
LGE				
LGE presence	162 (68.9)	36 (80.0)	126 (66.3)	.07
LGE mass (g)	3.8 (0.8–11.5)	9.5 (2.6–27.0)	3.0 (0.4–10.1)	.001
LGE extent (%)	4.7 (0.9–14.2)	13.2 (2.8–22.5)	3.8 (0.7–10.8)	<.001
LGE localization				
LGE anterior	75 (31.9)	21 (46.7)	54 (28.4)	.02
LGE lateral	129 (54.9)	27 (60.0)	102 (53.7)	.44
LGE inferior	115 (48.9)	27 (60.0)	88 (46.3)	.10
LGE septal	114 (48.5)	28 (62.2)	86 (45.3)	.04
LGE RV	25 (10.6)	12 (26.7)	13 (6.8)	<.001
LGE pattern				
Subepicardial	107 (45.5)	19 (42.2)	88 (46.3)	.62
Intramyocardial	117 (49.8)	22 (48.9)	95 (50.0)	.89
Subendocardial	35 (14.9)	16 (35.6)	19 (10.0)	<.001
Transmural	24 (10.2)	15 (33.3)	9 (4.7)	<.001
T2 ratio	2.4 ± 0.9	2.4 ± 0.8	2.4 ± 0.9	.94
T2 mapping (msec)				
Global T2	56.5 ± 9.8	61.1 ± 10.0	55.3 ± 9.4	.03
T2 basal segment	54.8 ± 9.1	59.4 ± 8.3	53.6 ± 9.0	.02
T2 middle segment	55.8 ± 9.8	59.9 ± 9.1	54.7 ± 9.8	.04
T2 apical segment	58.1 ± 11.5	63.8 ± 12.8	56.6 ± 10.7	.02
T1 mapping (msec)				
Global native T1	1277 ± 59	1342 ± 64	1263 ± 48	<.001
Native T1 basal segment	1274 ± 66	1344 ± 68	1259 ± 55	<.001
Native T1 middle segment	1265 ± 62	1333 ± 65	1251 ± 50	<.001
Native T1 apical segment	1303 ± 60	1357 ± 65	1281 ± 53	.002
ECV (%)				
Global ECV	33.8 ± 6.8	39.1 ± 8.7	32.7 ± 5.7	<.001
ECV basal segment	33.5 ± 6.9	38.8 ± 8.4	32.3 ± 5.9	<.001
ECV middle segment	33.5 ± 7.1	37.9 ± 9.7	32.5 ± 6.0	.005
ECV apical segment	34.9 ± 7.6	39.9 ± 10.4	33.8 ± 6.4	.004

Note.—Data are presented as means ± SDs, medians with IQRs in parentheses, or numbers of patients with percentages in parentheses. ECV = extracellular volume fraction, LAD = left atrial diameter, LGE = late gadolinium enhancement, LVCI = left ventricular cardiac index, LVCO = left ventricular cardiac output, LVEDD = left ventricular end-diastolic diameter, LVEDVi = left ventricular end-diastolic volume index, LVEF = left ventricular ejection fraction, LVESVi = left ventricular end-systolic volume index, LVSV = left ventricular stroke volume, MACE = major adverse cardiovascular event, RV = right ventricle.

interviews in cases of events after the patient was discharged. For those patients who could not be reached by phone, information on events was obtained through their spouse or close relatives. The primary end point was a composite of MACEs, including cardiac death, heart failure hospitalization, heart transplantation, recurrent myocarditis after a symptom-free interval of more than 2 months after the initial presentation (13,14), and recorded sustained ventricular arrhythmia (>30 seconds). All cardiovascular events were adjudicated by an expert cardiovascular adjudication committee blinded to the cardiac MRI data.

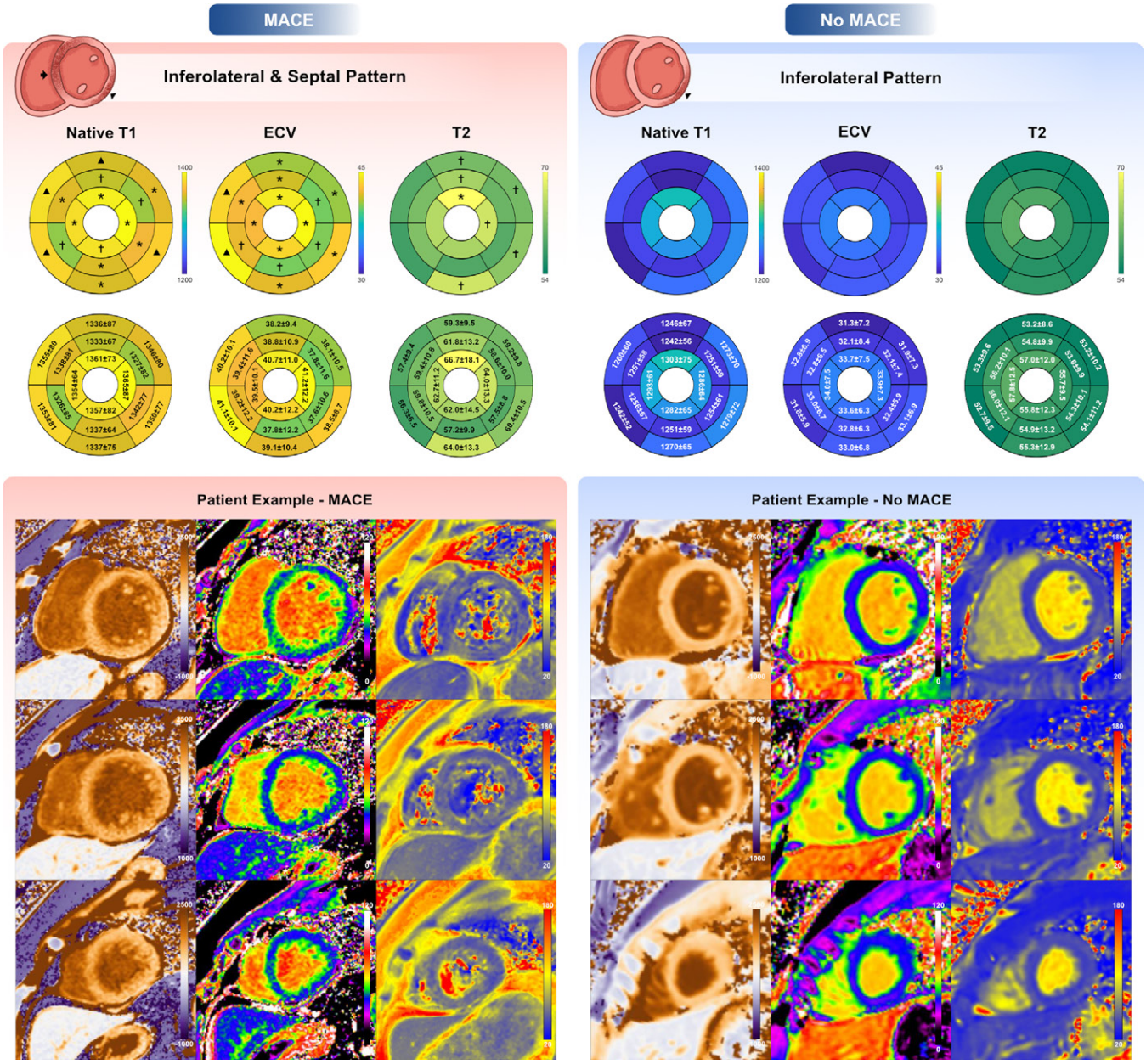

Figure 3: Bull's-eye diagrams show the segmental comparison of native T1, extracellular volume fraction (ECV), and T2 between the group with major adverse cardiovascular events (MACEs) and the group without MACEs. In addition to the typical distribution pattern of myocarditis with cardiac tissue abnormalities in the inferolateral wall, the group with MACEs also shows elevated native T1, ECV, and T2 in the ventricular septum and anterior wall. Lower left pictures: native T1 images (left column), ECV fraction images (middle column), and native T2 images (right column) in a 26-year-old male patient with acute myocarditis, with native T1, ECV, and T2 of 35.4%, 1337 msec, and 53.8 msec, respectively. The patient experienced a recurrent episode of acute myocarditis 556 days after cardiac MRI scan. Lower right pictures: native T1 images (left column), ECV fraction images (middle column), and native T2 images (right column) in a 19-year-old male patient with acute myocarditis, with native T1, ECV, and T2 of 30.9%, 1279 msec, and 51.5 msec, respectively. This patient was without the event of interest at the last follow-up (577 days after cardiac MRI scan). † = $P < .05$; * = $P < .01$; ▲ = $P < .001$.

Statistical Analysis

Statistical analysis was performed using SPSS software (version 26.0; IBM) and R software (version 4.3.1; R Foundation for Statistical Computing). Normally distributed data are presented as means ± SDs, nonnormally distributed data as medians (IQRs), and dichotomous variables as frequencies and percentages. The study cohort was divided into two groups based on the presence or absence of MACEs for a subgroup analysis. Categorical variables were compared using the Pearson χ^2 test or Fisher exact test, whereas comparisons for continuous data were performed using the Student *t* test (normal distribution data) or Wilcoxon rank sum test (nonnormal distribution data). Time to event was calculated from the date of cardiac MRI to the date of event or last follow-up (unit in days). Patients without the event of interest were censored at the date of their last follow-up. Kaplan-Meier survival estimates were calculated for each group of patients along with a log-rank test. Univariable Cox proportional hazard models were used to test the association between the end points and baseline covariates (hazard ratio [HR] and 95% CI). We incorporated variables with $P < .05$ in the univariable analysis into the multivariable analysis, with risk factors that had been reported in previous studies (5,14,23) and those with $P < .001$ being prioritized. Variables

Table 3: Univariable Cox Regression Analysis for Association of Variables with MACEs

Parameter	HR (95% CI)	*P* Value
Demographics		
Age (y)	1.03 (1.00, 1.05)	.03
Male sex	0.78 (0.43, 1.41)	.41
Body mass index	0.98 (0.92, 1.05)	.58
Clinical presentation		
Infarctlike presentation	0.29 (0.14, 0.59)	.001
Heart failure presentation	2.90 (1.60, 5.28)	<.001
Arrhythmia presentation	1.10 (0.51, 2.36)	.81
Cardiac function		
NYHA I–II	0.36 (0.20, 0.64)	.001
NYHA III–IV	2.81 (1.56, 5.06)	.001
Cardiac MRI quantification of function and structure		
LVEF (%)	0.95 (0.93, 0.97)	<.001
LVEF (per 5% increase)	0.77 (0.70, 0.84)	<.001
LVEF < 40%	6.67 (3.68, 12.10)	<.001
LVEDVi (mL/m^2)	1.02 (1.01, 1.03)	<.001
LVESVi (mL/m^2)	1.02 (1.01, 1.03)	<.001
LVSV (mL)	0.97 (0.96, 0.99)	<.001
LVCI (L/min/m^2)	0.62 (0.41, 0.95)	.03
LVCO (L/min)	0.73 (0.59, 0.91)	.005
Left ventricle mass (g)	1.00 (0.99, 1.01)	.41
LGE		
LGE presence	1.81 (0.87, 3.75)	.11
LGE mass (g)	1.04 (1.02, 1.07)	<.001
LGE extent (%)	1.05 (1.03, 1.07)	<.001
LGE localization		
LGE anterior	1.90 (1.05, 3.41)	.03
LGE lateral	1.18 (0.65, 2.15)	.58
LGE inferior	1.51 (0.830, 0.74)	.18
LGE septal	1.97 (1.08, 3.60)	.03
LGE RV	4.45 (2.28, 8.67)	<.001
LGE pattern		
Subepicardial	0.82 (0.45, 1.49)	.52
Intramyocardial	0.98 (0.55, 1.76)	.94
Subendocardial	4.19 (2.27, 7.73)	<.001
Transmural	6.24 (3.35, 11.63)	<.001
T2 ratio	0.93 (0.67, 1.28)	.64
T2 mapping		
Global T2	1.06 (1.02, 1.09)	.002
Global T2 (per 3-msec increase)	1.17 (1.05, 1.30)	.005
T2 basal segment	1.05 (1.01, 1.08)	.01
T2 middle segment	1.04 (1.00, 1.08)	.08
T2 apical segment	1.04 (1.01, 1.08)	.03
T1 mapping		
Global native T1	1.13 (1.07, 1.18)	<.001
Global native T1 (per 10-msec increase)	1.77 (1.41, 2.23)	<.001
Native T1 basal segment	1.12 (1.07, 1.18)	<.001
Native T1 middle segment	1.09 (1.03, 1.15)	.002
Native T1 apical segment	1.08 (1.02, 1.13)	.006
ECV		
Global ECV	1.13 (1.08, 1.18)	<.001
Global ECV (per 5% increase)	1.85 (1.47, 2.32)	<.001
ECV basal segment	1.14 (1.09, 1.20)	<.001
ECV middle segment	1.11 (1.07, 1.16)	<.001
ECV apical segment	1.10 (1.06, 1.14)	<.001

Note.—Body mass index is calculated as weight in kilograms divided by height in meters squared. ECV = extracellular volume fraction, HR = hazard ratio, LGE = late gadolinium enhancement, LVCI = left ventricular cardiac index, LVCO = left ventricular cardiac output, LVEDVi = left ventricular end-diastolic volume index, LVEF = left ventricular ejection fraction, LVESVi = left ventricular end-systolic volume index, LVSV = left ventricular stroke volume, MACE = major adverse cardiovascular event, NYHA = New York Heart Association, RV = right ventricle.

that shared collinearity with others were excluded by collinearity diagnostics (variance inflation factor and tolerance). Considering the conservative convention of at least 10 outcome events for each predictor variable, we included up to four variables in the multivariable Cox regression model. For each variable in the multivariable Cox regression model, tolerance values were greater than 0.2, and values of variance inflation factor were less than 3. Finally, we combined the best performing parameters to create risk model 1: heart failure presentation, cardiac function parameters (LVEF per 5% increase), and conventional imaging parameter (LGE extent). Models 2 and 3 were created by adding native T1 (model 2) and ECV (model 3) to the model 1 parameters, creating parsimonious models containing the strongest predictive variables. The prognostic capability of stepwise models with sequentially included variables was evaluated by the goodness of fit, indicated by χ^2 test, and compared with the subsequent model by means of likelihood ratio test and Harrell C statistics. The model with the lowest Akaike information criterion value was chosen as the best fitting model. Robustness testing was carried out to assess the model's stability against variations in datasets using the bootstrap method with 1000 resampling cycles. For variables with missing values (all < 5%), single imputation procedures were performed. Variables with missing values were excluded from the multivariable analysis. Two-tailed $P < .05$ was considered significant.

The inter- and intraobserver variabilities for native T1, ECV, and T2 values were evaluated using the intraclass correlation coefficient in a randomly selected subgroup of 20 patients (Appendix S1). One observer (Y.W.) performed one measurement, and a second observer (M.L.) blinded to the first observer's results performed measurements at two time points at least 1 week apart.

Results

Study Sample Characteristics

The final analysis included 235 patients (mean age: 32 years ± 13 [SD]; 63.8% [*n* = 150] men; 36.2% [*n* = 85] women)

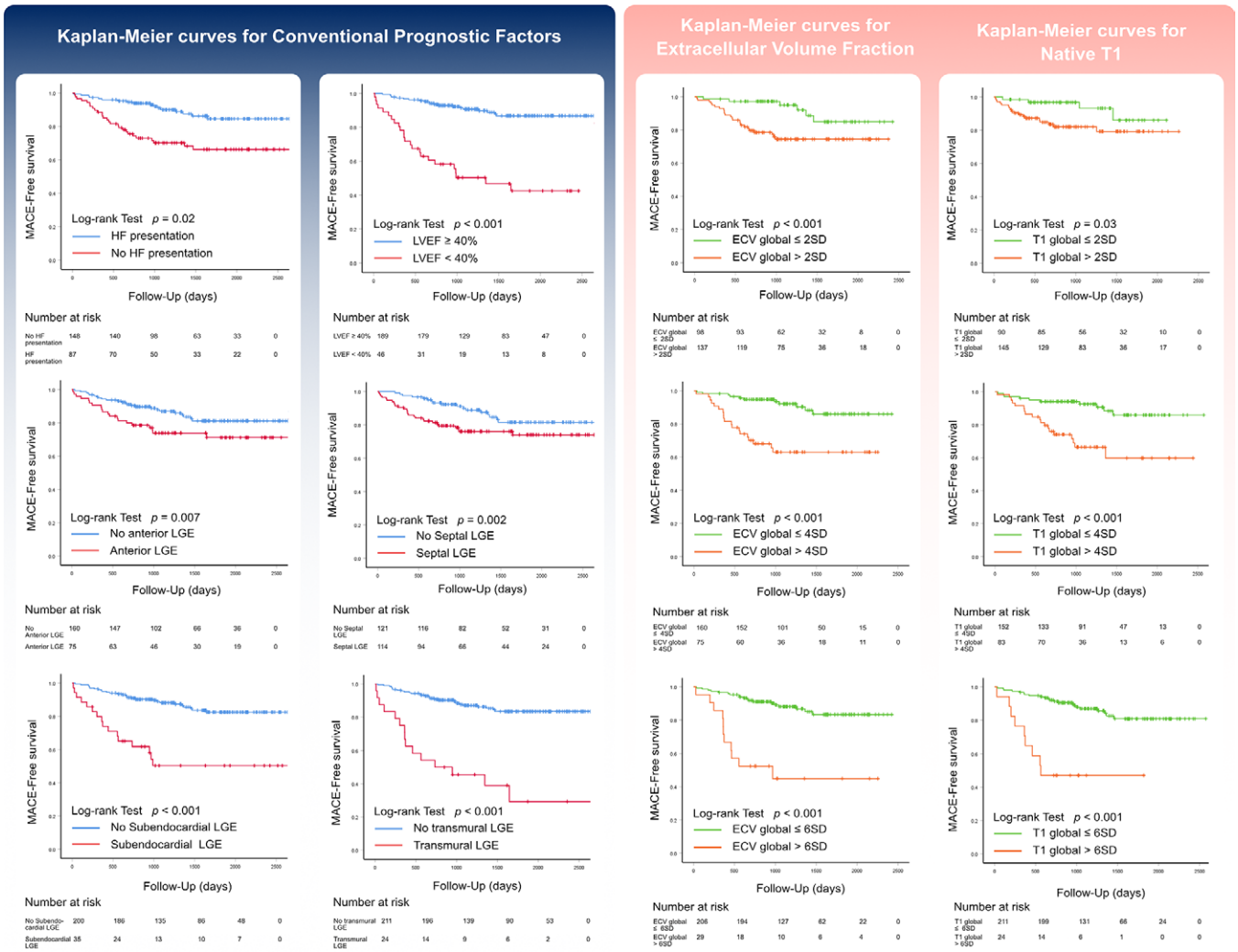

Figure 4: Kaplan-Meier curves for major adverse cardiovascular events (MACEs) in patients with myocarditis. Kaplan-Meier curves for conventional prognostic factors, extracellular volume fraction (ECV), and native T1. HF = heart failure, LVEF = left ventricular ejection fraction, LGE = late gadolinium enhancement.

(Fig 1, Table 1). The latest follow-up date was May 2024 with a median follow-up time of 1637 days (IQR: 1441–1833 days). Of the 235 patients, 45 (19%) patients experienced MACEs, encompassing hospitalization for heart failure (n = 15; 6.4%), sustained ventricular tachycardia (n = 8; 3.4%), cardiac death (n = 11; 4.7%), recurrent myocarditis (n = 9; 3.8%), or heart transplantation (n = 2; 0.9%). The pathology results and intraclass correlation coefficient results are described in Appendix S1 and Tables S1 and S2.

Clinical and Cardiac MRI Characteristics Based on the Presence of MACEs

Detailed patient baseline information and cardiac MRI characteristics are presented in Tables 1 and 2. The median number of days of symptoms before cardiac MRI was 13 days (IQR: 7–20 days). The most common clinical presentation was infarctlike symptoms such as chest pain (n = 110; 46.8%) and heart failure presentation such as dyspnea (n = 87; 37.0%), the latter being more common in patients with MACEs. Compared with the other group, patients with MACEs had higher high-sensitivity cardiac troponin I and N-terminal pro–brain natriuretic peptide (NT-proBNP) value (0.128 ng/mL vs 0.064 ng/mL; P = .02; 1300.5 ng/L vs 240.0 ng/L; P < .001, respectively). Patients with MACEs had worse cardiac function with lower LVEF (39.4% ± 16.5 vs 53.6% ± 12.0; P < .001) and higher LV end-systolic volume index (69.0 mL/m^2 ± 41.4 vs 39.9 mL/m^2 ± 24.0; P < .001). Patients in this group also had increased levels of left atrial diameter (34.5 mm ± 9.3 vs 26.8 mm ± 6.8; P < .001) and LV end-diastolic diameter (54.8 mm ± 8.8 vs 50.9 mm ± 7.5; P = .002). LV stroke volume, LV cardiac index, and LV cardiac output in the group with MACEs were lower than those in the group without MACEs (62.9 mL ± 20.2 vs 77.0 mL ± 22.5; P < .001; 2.7 L/min/m^2 ± 0.7 vs 3.0 L/min/m^2 ± 0.8; P = .01; 4.6 L/min ± 1.5 vs 5.5 L/min ± 1.7; P = .002, respectively).

Of all the 235 patients, 162 (68.9%) had positive LGE, with significant differences in the distribution and pattern of enhancement between the two groups. The group with MACEs had greater LGE burden with 13.2% LGE of the LV mass versus 3.8% LGE in the group without MACEs (P < .001). Anterior LGE, septal LGE, right ventricle LGE, subendocardial LGE, and transmural LGE were more frequently observed in patients with MACEs (47% [21 of 45] vs 28.4% [54 of 190]; P = .02; 62% [28 of 45] vs 45.3% [86 of 190]; P = .04; 27% [12 of 45] vs

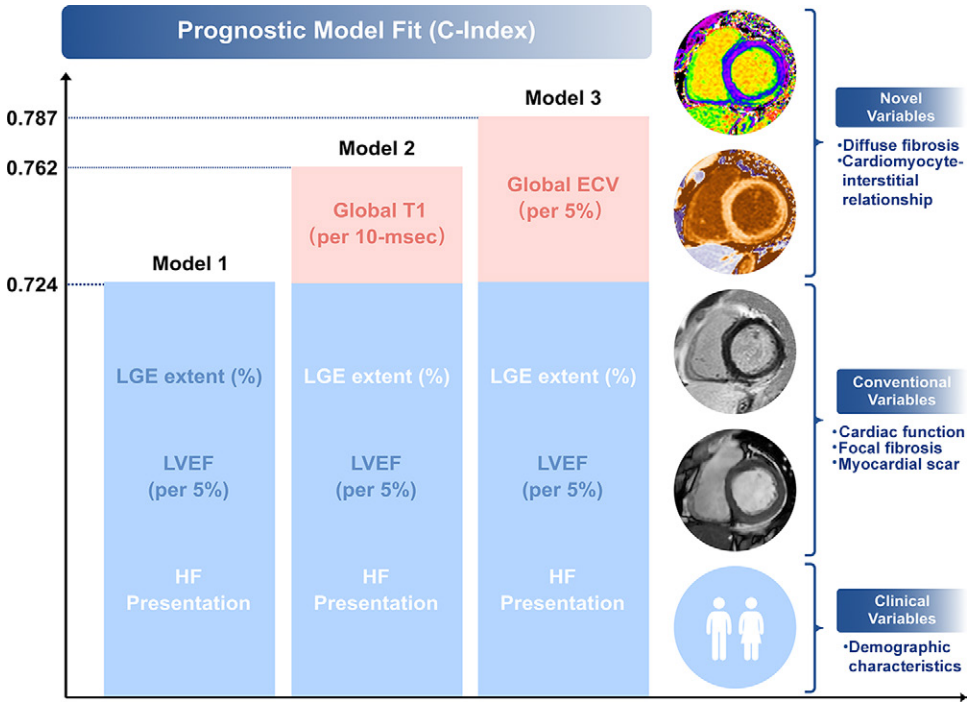

Figure 5: Prognostic significance of myocardial parametric mapping in patients with myocarditis. Cox regression analysis demonstrated the incremental predictive role of native T1 (model 2) and extracellular volume fraction (ECV) (model 3) for the identification of patients with acute myocarditis independent of clinical variables, left ventricular ejection fraction (LVEF), and late gadolinium enhancement (LGE). HF = heart failure.

6.8% [13 of 190]; $P < .001$; 36% [16 of 45] vs 10.0% [19 of 190]; $P < .001$; 33% [15 of 45] vs 4.7% [nine of 190]; $P < .001$, respectively). The global native T1, ECV, and T2 values were significantly higher in the group with MACEs compared with the group without MACEs (1342 msec ± 64 vs 1263 msec ± 48; $P < .001$; 39.1% ± 8.7 vs 32.7% ± 5.7; $P < .001$; 61.1 msec ± 10.0 vs 55.3 msec ± 9.4; $P = .03$, respectively). In addition to the typical distribution pattern of myocarditis with cardiac tissue abnormalities in the inferolateral wall, the group with MACEs also showed elevated native T1, ECV, and T2 in the ventricular septum and anterior wall (Fig 3).

Predictors of MACEs

In univariable Cox regression analyses, multiple factors were associated with MACEs, including clinical parameters (age, heart failure presentation, New York Heart Association function class III–IV, log N-terminal pro–brain natriuretic peptide), cardiac MRI tissue characteristics (LGE extent, anterior LGE, septal LGE, right ventricle LGE, subendocardial LGE, and transmural LGE), cardiac MRI cardiac function and dimensions (LVEF, LV end-diastolic volume index, LV end-systolic volume index, LV stroke volume, cardiac index, and cardiac output), and quantitative relaxation parameters (Table 3 and Table S3). LGE presence was not a significant predictor of MACEs (HR: 1.81; 95% CI: 0.87, 3.75; $P = .11$). Global native T1, ECV, and T2 were independently associated with MACEs (HR: 1.13 [95% CI: 1.07, 1.18]; $P < .001$; HR: 1.13 [95% CI: 1.08, 1.18]; $P < .001$; HR: 1.06 [95% CI: 1.02, 1.09]; $P = .002$, respectively). Diagnosis of giant cell myocarditis by endomyocardial biopsy was also associated with increased risk of MACEs ($P < .001$) (Table S2). The prognostic value of most parameters was comparable between patients with infarctlike presentation and those with heart failure presentation; however, LGE burden and specific LGE pattern were significant predictors of MACEs only in the heart failure group (Table S4). Kaplan-Meier survival curves showed that patients with heart failure presentation; an LVEF of less than 40%; septal LGE; anterior LGE; transmural LGE; native T1; or ECV higher than the mean plus 2 SDs, 4 SDs, and 6 SDs had a significantly higher incidence of MACEs (Fig 4). LGE extent demonstrated prognostic significance in the univariable Cox analysis and multivariate Cox analysis (HR: 1.05 [95% CI: 1.03, 1.07]; $P < .001$; HR: 1.03 [95% CI: 1.00, 1.05]; $P = .04$). Global native T1, ECV, and T2 all were associated with increased risk of MACEs. Multivariate analysis confirmed that native T1 (HR: 1.61; 95% CI: 1.31, 1.98; $P < .001$) and ECV (HR: 1.70; 95% CI: 1.38, 2.08; $P < .001$) were independent prognostic factors (Table 4; Figs 5, 6). However, T2 did not show independent prognostic value according to multivariable Cox regression analysis (Table S5). The Harrell C index for model 2—including native T1 (per 10-msec increase) in addition to LVEF (per 5% increase), clinical variables, and LGE extent to predict MACEs—was 0.76, which was significantly higher than that for model 1, which did not include native T1 (Harrell C index = 0.72). By adding ECV (per 5% increase) to model 1, the model Harrell C index increased to 0.79. The Akaike information criterion values for models 1–3 were 434.3, 421.3, and 415.8, respectively, with model 3 being the best performing model.

Discussion

This study of a relatively large cohort of patients with acute myocarditis had several important findings that deepen our understanding of the clinical and cardiac MRI characteristics of these patients, particularly in the context of associations

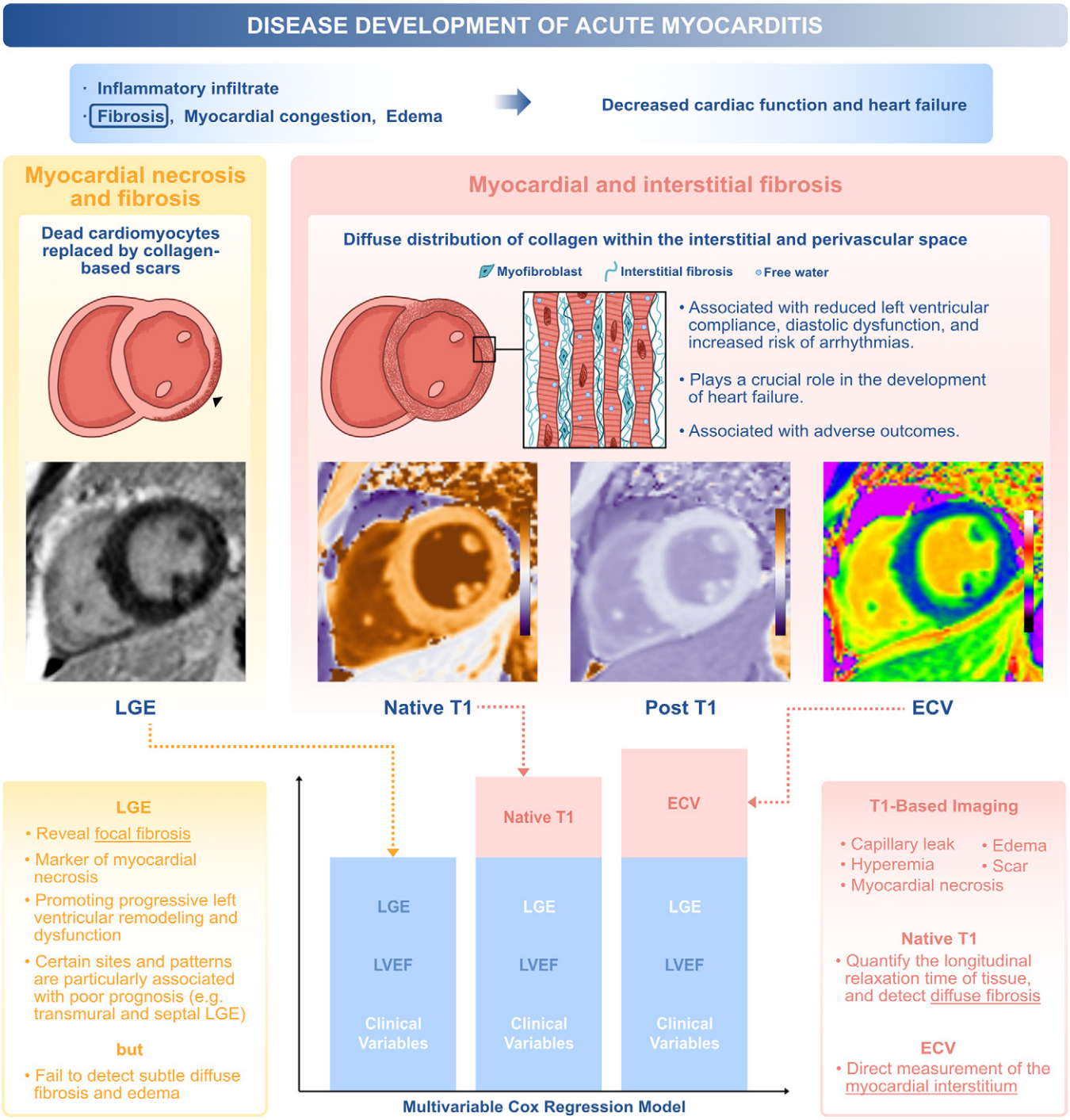

Figure 6: Myocardial tissue alterations quantified by myocardial parametric mapping are powerful prognostic factors in myocarditis. This study shows the potential of using myocardial parametric mapping to predict prognosis. In a series of multivariable Cox regression models, the addition of global extracellular volume fraction (ECV) (model 3) and global native T1 (model 2) improved prognostication compared with model 1 including only clinical variables, left ventricular ejection fraction (LVEF), and late gadolinium enhancement (LGE) extent. Myocardial fibrosis is characterized by the expansion of the cardiac interstitium through the deposition of extracellular matrix proteins, which also occurs in the disease progression of myocarditis. Fibrosis leads to myocardial stiffness and conduction system abnormalities that perturb systolic and diastolic function and is thought to play an important role in the pathogenesis of cardiac arrhythmias. LGE is a robust technique for identifying myocardial necrosis and scarring but is not sufficiently sensitive to detect diffuse fibrosis and edema. Myocardial parametric mapping enables quantitative assessment of the myocardium and compensates for the shortcomings of conventional techniques. T1 mapping can reflect pathologic changes in both myocardium and interstitium and identify diffuse fibrosis at an early stage. The measurement of myocardial extracellular volume by ECV will further contribute to understanding the pathophysiology of heart disease and will guide the development of effective therapeutic approaches.

between myocardial parametric mapping parameters and MACEs. First, we observed that a substantial proportion of patients experienced MACEs (19%) during the median follow-up period. The array of events, ranging from heart failure hospitalization to heart transplantation, underscores the potential severity of acute myocarditis and its diverse clinical outcomes. Second, we found a strong association between various clinical and cardiac MRI parameters with MACEs, elucidating the role of specific cardiac MRI characteristics, cardiac functions, and quantitative relaxation parameters in predict-

Table 4: Multivariable Cox Regression Analysis for Association of Variables with MACEs

Parameter	HR (95% CI)	*P* Value
Model 1 covariates		
Heart failure presentation	…	…
LVEF (per 5% increase)	0.79 (0.72, 0.88)	<.001
LGE extent (%)	1.03 (1.00, 1.05)	.04
Model 2 covariates		
Heart failure presentation	…	…
LVEF (per 5% increase)	0.81 (0.73, 0.89)	<.001
LGE extent (%)	…	…
Global native T1 (per 10-msec increase)	1.61 (1.31, 1.98)	<.001
Model 3 covariates		
Heart failure presentation	…	…
LVEF (per 5% increase)	0.81 (0.73, 0.90)	<.001
LGE extent (%)	…	…
Global ECV (per 5% increase)	1.70 (1.38, 2.08)	<.001

Note.—ECV = extracellular volume fraction, HR = hazard ratio, LGE = late gadolinium enhancement, LVEF = left ventricular ejection fraction, MACE = major adverse cardiovascular event.

ing MACEs. Third, the addition of native T1 and ECV to the baseline model, including conventional parameters, increased the Harrell C index from 0.72 to 0.79. The progressively enhanced predictive capability of the constructed models emphasizes the value of incorporating quantitative mapping parameters into risk assessment for MACEs.

The prognostic role of LGE in myocarditis has been confirmed by an increasing number of research studies to have strong prognostic potential (8). However, in this study, LGE presence was not a significant predictor of MACEs. We believe this may be attributed to our reporting of the presence or absence of LGE as a binary variable and the relatively high percentage of patients positive for LGE (68.9%). Analyses using binary or categorical variables tend to have lower power compared with continuous variables (24). Furthermore, previous studies reporting the statistical significance of LGE in Cox analysis tend to have a lower percentage of patients with LGE (28.3%, 44%, 62.2%) (6,25,26). Conversely, studies with a higher proportion of patients with LGE (80%, 93%) exhibited similar results to ours, with LGE presence demonstrating a nonsignificant increased incidence of adverse events (11,27). As expected, LGE extent demonstrated prognostic significance in the multivariate Cox analysis. Still, LGE presents certain limitations. It may not effectively detect subtle, diffuse fibrosis (28). More sensitive methods are needed to detect subtle and diffuse changes in myocardial tissue.

T1 mapping offers a quantitative approach, providing mean T1 relaxation times within individual voxels, making it a valuable alternative for quantifying diffuse myocardial fibrosis (29). Furthermore, T1 mapping offers comprehensive myocardial characterization, encompassing parameters related to edema, myocyte expansion, and iron deposition, providing additional insights into cardiac pathophysiology (30). When T1 mapping is conducted both before and after the administration of gadolinium-based contrast agent, the ECV fraction, which is a direct measurement of the size of the extracellular space, can be calculated after correction for hematocrit. Our findings are consistent with previous articles that native T1 and ECV are highly valuable independent predictors of adverse cardiovascular outcomes (10).

However, T1 mapping techniques may be method and vendor dependent and are affected by tissue edema, hyperemia, and capillary leak. Unlike native T1, ECV assesses the interstitium as a proportion of the total LV myocardial volume and is relatively independent of field strength, thus providing an added advantage (31). Interstitial and perivascular fibrosis generally leads to a reduction in LV compliance and adversely affects diastolic function, with its effects on systolic function being comparatively lesser or manifesting later in the disease course (32). Cardiac MRI parametric mapping is more sensitive to detect interstitial fibrosis, which represents the primary injury process (33). We believe this is the reason why model 3, including ECV in addition to native T1 and conventional parameters, had the best prognosis among all models. The division of the myocardium into interstitium and cardiomyocytes, rather than a homogeneous tissue, has been emphasized in recent years (34). The measurement of myocardial extracellular volume by ECV will further contribute to understanding the pathophysiology of heart disease and will guide the development of effective therapeutic approaches.

Myocardial edema is an important pathophysiologic component of acute myocarditis, as evidenced by elevated intracellular and interstitial free water in the myocardium (35). It not only affects cardiac function and ventricular compliance but may also lead to arrhythmias (36). Quantitative T2 mapping is capable of detecting diffuse myocardial edema and assessing the severity of tissue damage without the use of contrast media (37). However, myocardial edema represents different clinical and prognostic significance in different diseases, and its presence does not necessarily correlate with a poor outcome. Aquaro et al (38) performed baseline and repeat cardiac MRI in patients with myocarditis and found that the presence of LGE without edema at follow-up was associated with a poorer prognosis, whereas the presence of edema indicated active inflammation of the myocardial tissue, with a chance of a full recovery. In acute myocarditis, the presence of edema may have both protective and harmful effects, which may explain why the T2 value was an independent prognostic factor in the univariable Cox analysis but not multivariable analysis in our study. The dynamic pathophysiology of myocardial edema in acute myocarditis still needs to be further explored.

This study had limitations. First, this study has potential selection bias inherent in retrospective studies. Not all patients with suspected myocarditis who came to our hospital underwent cardiac MRI, and our results may not be generalizable. However, as a matter of routine clinical practice at our institution, patients with suspected myocarditis are referred for cardiac MRI unless there are contraindications. Second, only a proportion of patients underwent endomyocardial biopsy, which remains the reference standard for the diagnosis of myocarditis. However, with the advent of the updated Lake Louise criteria, cardiac MRI is increasingly applied instead of endomyocardial biopsy to diagnose acute myocarditis in many centers. All patients included in this study had clinical features consistent with myocarditis, with symptomatic relief after receiving treatment, which indirectly confirmed the diagnosis. Finally, due to the low prevalence of myocarditis and the small number of events, it was also not possible to perform

subgroup analyses to evaluate the prognostic role of the mapping technique in patients without LGE. It is hoped that the results of this work will inspire future studies to address these issues.

In conclusion, this comprehensive study delineates the value of cardiac MRI in the nuanced diagnosis and prognostication of myocarditis. Cox regression models combining advanced quantitative cardiac MRI parameters, in particular native T1 mapping and ECV, with conventional parameters showed improved performance in predicting MACEs compared with the baseline model. Future research should focus on the role of cardiac MRI parametric mapping in guiding long-term management for patients with myocarditis, with an emphasis on integrating these techniques into broader clinical workflows.

Author affiliations:

[1] Department of Magnetic Resonance Imaging, Fuwai Hospital, State Key Laboratory of Cardiovascular Disease, National Center for Cardiovascular Diseases, Chinese Academy of Medical Sciences and Peking Union Medical College, Beijing 100037, China

[2] Department of Pathology, Fuwai Hospital, State Key Laboratory of Cardiovascular Disease, National Center for Cardiovascular Diseases, Chinese Academy of Medical Sciences and Peking Union Medical College, Beijing, China

[3] Department of Health and Human Services, National Heart, Lung and Blood Institute, National Institutes of Health, Bethesda, Md

[4] Johns Hopkins Medicine-Suburban Hospital, Kensington, Md

[5] Division of Cardiovascular Medicine, University of Utah School of Medicine, Salt Lake City, Utah

[6] Key Laboratory of Cardiovascular Imaging (Cultivation), Chinese Academy of Medical Sciences, Beijing, China

Received April 3, 2024; revision requested April 25; revision received October 18; accepted December 24.

Address correspondence to: M.L. (email: coolkan@163.com).

Funding: Supported by The Construction Research Project of the Key Laboratory (Cultivation) of Chinese Academy of Medical Sciences (2019PT310025); National Natural Science Foundation of China (82471973); Noncommunicable Chronic Diseases-National Science and Technology Major Project (2023ZD0504502); Chinese Academy of Medical Sciences Innovation Fund for Medical Sciences (CIFMS, 2021-I2M-1-063); Clinical and Translational Fund of Chinese Academy of Medical Sciences (2019XK320063); Youth Key Program of High-level Hospital Clinical Research (2022-GSP-QZ-5).

Author contributions: Guarantors of integrity of entire study, **X.D., M.L.**; study concepts/study design or data acquisition or data analysis/interpretation, all authors; manuscript drafting or manuscript revision for important intellectual content, all authors; approval of final version of submitted manuscript, all authors; agrees to ensure any questions related to the work are appropriately resolved, all authors; literature research, **Y.W., X.D., J.X., D.Z., W.Y., M.J., A.E.A., S.Z., M.L.**; clinical studies, **Y.W., X.D., L.Z., J.X., D.Z., H.W., M.L.**; statistical analysis, **Y.W., X.D., J.X., D.Z., M.L.**; and manuscript editing, **Y.W., X.D., D.Z., W.Y., A.S., A.E.A., H.W., M.L.**

Disclosures of conflicts of interest: Y.W. The Construction Research Project of the Key Laboratory (Cultivation) of Chinese Academy of Medical Sciences (2019PT310025); National Natural Science Foundation of China (81971588); Clinical and Translational Fund of Chinese Academy of Medical Sciences (2019XK320063); Youth Key Program of High-level Hospital Clinical Research (2022-GSP-QZ5). **X.D.** No relevant relationships. **L.Z.** No relevant relationships. **J.X.** No relevant relationships. **D.Z.** No relevant relationships. **W.Y.** No relevant relationships. **M.J.** No relevant relationships. **H.Z.** No relevant relationships. **A.S.** No relevant relationships. **A.E.A.** Licenses or royalties from Circle CVi; payment or honoraria from Bayer and Circle CVi. **S.Z.** No relevant relationships. **H.W.** No relevant relationships. **M.L.** No relevant relationships.

References

1. Ammirati E, Moslehi JJ. Diagnosis and Treatment of Acute Myocarditis: A Review. JAMA 2023;329(13):1098–1113.
2. D'Ambrosio A, Patti G, Manzoli A, et al. The fate of acute myocarditis between spontaneous improvement and evolution to dilated cardiomyopathy: a review. Heart 2001;85(5):499–504.
3. Kotanidis CP, Bazmpani MA, Haidich AB, Karvounis C, Antoniades C, Karamitsos TD. Diagnostic Accuracy of Cardiovascular Magnetic Resonance in Acute Myocarditis: A Systematic Review and Meta-Analysis. JACC Cardiovasc Imaging 2018;11(11):1583–1590.
4. Yang F, Wang J, Li W, et al. The prognostic value of late gadolinium enhancement in myocarditis and clinically suspected myocarditis: systematic review and meta-analysis. Eur Radiol 2020;30(5):2616–2626.
5. Georgiopoulos G, Figliozzi S, Sanguineti F, et al. Prognostic Impact of Late Gadolinium Enhancement by Cardiovascular Magnetic Resonance in Myocarditis: A Systematic Review and Meta-Analysis. Circ Cardiovasc Imaging 2021;14(1):e011492.
6. Gräni C, Eichhorn C, Bière L, et al. Prognostic Value of Cardiac Magnetic Resonance Tissue Characterization in Risk Stratifying Patients With Suspected Myocarditis. J Am Coll Cardiol 2017;70(16):1964–1976 [Published correction appears in J Am Coll Cardiol 2017;70(21):2736.].
7. Karamitsos TD, Arvanitaki A, Karvounis H, Neubauer S, Ferreira VM. Myocardial Tissue Characterization and Fibrosis by Imaging. JACC Cardiovasc Imaging 2020;13(5):1221–1234.
8. Eichhorn C, Greulich S, Bucciarelli-Ducci C, Sznitman R, Kwong RY, Gräni C. Multiparametric Cardiovascular Magnetic Resonance Approach in Diagnosing, Monitoring, and Prognostication of Myocarditis. JACC Cardiovasc Imaging 2022;15(7):1325–1338.
9. Carbone I, Friedrich MG. Myocardial edema imaging by cardiovascular magnetic resonance: current status and future potential. Curr Cardiol Rep 2012;14(1):1–6.
10. Gräni C, Bière L, Eichhorn C, et al. Incremental value of extracellular volume assessment by cardiovascular magnetic resonance imaging in risk stratifying patients with suspected myocarditis. Int J Cardiovasc Imaging 2019;35(6):1067–1078.
11. Spieker M, Haberkorn S, Gastl M, et al. Abnormal T2 mapping cardiovascular magnetic resonance correlates with adverse clinical outcome in patients with suspected acute myocarditis. J Cardiovasc Magn Reson 2017;19(1):38.
12. Thavendiranathan P, Zhang L, Zafar A, et al. Myocardial T1 and T2 Mapping by Magnetic Resonance in Patients With Immune Checkpoint Inhibitor-Associated Myocarditis. J Am Coll Cardiol 2021;77(12):1503–1516.
13. Caforio ALP, Pankuweit S, Arbustini E, et al. Current state of knowledge on aetiology, diagnosis, management, and therapy of myocarditis: a position statement of the European Society of Cardiology Working Group on Myocardial and Pericardial Diseases. Eur Heart J 2013;34(33):2636–2648, 2648a–2648d.
14. Bernhard B, Schnyder A, Garachemani D, et al. Prognostic Value of Right Ventricular Function in Patients With Suspected Myocarditis Undergoing Cardiac Magnetic Resonance. JACC Cardiovasc Imaging 2023;16(1):28–41.
15. Li JH, Xu XQ, Zhu YJ, et al. Subendocardial Involvement as an Underrecognized Cardiac MRI Phenotype in Myocarditis. Radiology 2022;302(1):61–69.
16. Messroghli DR, Radjenovic A, Kozerke S, Higgins DM, Sivananthan MU, Ridgway JP. Modified Look-Locker inversion recovery (MOLLI) for high-resolution T1 mapping of the heart. Magn Reson Med 2004;52(1):141–146.
17. Li S, Zhou D, Sirajuddin A, et al. T1 Mapping and Extracellular Volume Fraction in Dilated Cardiomyopathy: A Prognosis Study. JACC Cardiovasc Imaging 2022;15(4):578–590.
18. Bönner F, Janzarik N, Jacoby C, et al. Myocardial T2 mapping reveals age- and sex-related differences in volunteers. J Cardiovasc Magn Reson 2015;17(1):9.
19. Schulz-Menger J, Bluemke DA, Bremerich J, et al. Standardized image interpretation and post-processing in cardiovascular magnetic resonance - 2020 update: Society for Cardiovascular Magnetic Resonance (SCMR): Board of Trustees Task Force on Standardized Post-Processing. J Cardiovasc Magn Reson 2020;22(1):19.
20. Messroghli DR, Moon JC, Ferreira VM, et al. Clinical recommendations for cardiovascular magnetic resonance mapping of T1, T2, T2* and extracellular volume: A consensus statement by the Society for Cardiovascular Magnetic Resonance (SCMR) endorsed by the European Association for Cardiovascular Imaging (EACVI). J Cardiovasc Magn Reson 2017;19(1):75. [Published correction appears in J Cardiovasc Magn Reson 2018;20(1):9.]
21. Puntmann VO, Carr-White G, Jabbour A, et al. T1-Mapping and Outcome in Nonischemic Cardiomyopathy: All-Cause Mortality and Heart Failure. JACC Cardiovasc Imaging 2016;9(1):40–50. [Published correction appears in JACC Cardiovasc Imaging 2017;10(3):384.]
22. Puntmann VO, Carr-White G, Jabbour A, et al. Native T1 and ECV of Noninfarcted Myocardium and Outcome in Patients With Coronary Artery Disease. J Am Coll Cardiol 2018;71(7):766–778.
23. Ammirati E, Cipriani M, Moro C, et al. Clinical Presentation and Outcome in a Contemporary Cohort of Patients With Acute Myocarditis: Multicenter Lombardy Registry. Circulation 2018;138(11):1088–1099.
24. Altman DG, Royston P. The cost of dichotomising continuous variables. BMJ 2006;332(7549):1080.
25. Schumm J, Greulich S, Wagner A, et al. Cardiovascular magnetic resonance risk stratification in patients with clinically suspected myocarditis. J Cardiovasc Magn Reson 2014;16(1):14.
26. Lee JW, Jeong YJ, Lee G, et al. Predictive Value of Cardiac Magnetic Resonance Imaging-Derived Myocardial Strain for Poor Outcomes in Patients with Acute Myocarditis. Korean J Radiol 2017;18(4):643–654.

27. Aquaro GD, Perfetti M, Camastra G, et al. Cardiac MR With Late Gadolinium Enhancement in Acute Myocarditis With Preserved Systolic Function: ITAMY Study. J Am Coll Cardiol 2017;70(16):1977–1987.
28. Perea RJ, Ortiz-Perez JT, Sole M, et al. T1 mapping: characterisation of myocardial interstitial space. Insights Imaging 2015;6(2):189–202.
29. Robinson AA, Chow K, Salerno M. Myocardial T1 and ECV Measurement: Underlying Concepts and Technical Considerations. JACC Cardiovasc Imaging 2019;12(11 Pt 2):2332–2344.
30. Liu A, Wijesurendra RS, Francis JM, et al. Adenosine Stress and Rest T1 Mapping Can Differentiate Between Ischemic, Infarcted, Remote, and Normal Myocardium Without the Need for Gadolinium Contrast Agents. JACC Cardiovasc Imaging 2016;9(1):27–36.
31. Gupta S, Ge Y, Singh A, Gräni C, Kwong RY. Multimodality Imaging Assessment of Myocardial Fibrosis. JACC Cardiovasc Imaging 2021;14(12):2457–2469.
32. Frangogiannis NG. Cardiac fibrosis. Cardiovasc Res 2021;117(6):1450–1488.
33. Gao XM, White DA, Dart AM, Du XJ. Post-infarct cardiac rupture: recent insights on pathogenesis and therapeutic interventions. Pharmacol Ther 2012;134(2):156–179.
34. Schelbert EB, Butler J, Diez J. Why Clinicians Should Care About the Cardiac Interstitium. JACC Cardiovasc Imaging 2019;12(11 Pt 2):2305–2318.
35. Friedrich MG. Myocardial edema--a new clinical entity? Nat Rev Cardiol 2010;7(5):292–296.
36. Desai KV, Laine GA, Stewart RH, et al. Mechanics of the left ventricular myocardial interstitium: effects of acute and chronic myocardial edema. Am J Physiol Heart Circ Physiol 2008;294(6):H2428–H2434.
37. Tada Y, Yang PC. Myocardial Edema on T2-Weighted MRI: New Marker of Ischemia Reperfusion Injury and Adverse Myocardial Remodeling. Circ Res 2017;121(4):326–328.
38. Aquaro GD, Ghebru Habtemicael Y, Camastra G, et al. Prognostic Value of Repeating Cardiac Magnetic Resonance in Patients With Acute Myocarditis. J Am Coll Cardiol 2019;74(20):2439–2448.